

# Objective and quantitative measurement of skin micro-relief by image analysis and application in age-dependent changes

Yue Wu<sup>1</sup>  | Toshiyuki Tanaka<sup>2</sup>

<sup>1</sup>Graduate School of Science and Technology, Keio University, Yokohama, Japan

<sup>2</sup>Faculty of Science and Technology, Keio University, Yokohama, Japan

## Correspondence

Toshiyuki Tanaka, Faculty of Science and Technology, Keio University, Yokohama, Japan.

Email: tanaka@appi.keio.ac.jp

## Abstract

**Background:** Skin micro-relief has been researched by a variety of devices and methods, which usually are expensive or complicated. On the other hand, skin micro-relief relates to quite a few parameters, and it is hard to evaluate all of them at the same time. In the study, all parameters related to skin micro-relief are extracted and evaluated by image analysis.

**Materials and Methods:** Skin micro-relief evaluation was divided into four aspects: (a) Tamura features method was used to evaluate skin surface. (b) Morphological transform was applied to extract skin pores. (c) Watershed transform was applied to extract skin furrows. (d) labeling operation was used to evaluate the number, area and average area of skin closed polygons. Then, cheek images from 163 healthy Japanese females (0-70 years old) are analyzed to explore the age-dependent changes.

**Results:** Most parameters increased as age went on with significant differences, such as skin surface coarseness, contrast, skin pore number, area, average area, skin furrow width, skin closed polygon area and skin closed polygon average area. Skin coarseness has a strong correlation with pore area.

**Conclusion:** The method proposed in the study provided a comprehensive and effective assessment of skin micro-relief.

## KEYWORDS

skin aging, skin pore, skin surface evaluation, skin texture, watershed transform

## 1 | INTRODUCTION

Human skin is the biggest organ in the body, which has a lot of characteristics and fundamental functions. On one hand, skin directly contacts the environment and can be influenced by chronological ages and environment changes, like humidity and temperature. On the other hand, skin can protect from Ultraviolet light. Skin is smooth, while the surface is not even due to the skin micro-relief, which is a pattern of the network consisting of furrows, polygonal

forms, and pores. (Figure 1). Skin micro-relief is one of the most important parameters of skin when mentioned in skin condition assessment and skin detection.

According to previous research, there are two main methods to evaluate skin micro-relief, which is using replica to get a copy of skin micro-relief, or using non-invasive devices to take the two-dimensional or three-dimensional images of skin micro-relief, like microscopy. These methods have their own merits. The replica can get the real and integrated topography of skin micro-relief, but it needs

This is an open access article under the terms of the Creative Commons Attribution-NonCommercial-NoDerivs License, which permits use and distribution in any medium, provided the original work is properly cited, the use is non-commercial and no modifications or adaptations are made.

© 2021 The Authors. *Skin Research and Technology* published by John Wiley & Sons Ltd.

to cover the material over the assessment position, which is inconvenient and not easy to operate. M. Akimoto et al,<sup>1</sup> used skin replica to get the copy of skin micro-relief, and then applied the image analysis method to measure the triangle area of the skin. Y. Masuda et al,<sup>2</sup> also used skin replica, however, they measured skin micro-relief according to the result of Confocal laser scanning microscopy. Commonly, three-dimensional images gotten needs professional and expensive equipment, like the PRIOR. Some two-dimensional images also need high resolution of the equipment, like skin microscopy. Campos et al,<sup>3</sup> explored the skin properties of oily skin, including skin micro-relief, in which skin pores are counted with Visioface<sup>®</sup> equipment which could obtain high-resolution images. Zou et al,<sup>4</sup> proposed a method to evaluate skin micro-relief by segmenting skin closed polygons and calculating their average area from two-dimensional images. C. Bontozoglou et al,<sup>5</sup> analyzed skin closed polygons and wrinkle length by skin capacitive images. C. I. Moon et al,<sup>6</sup> developed a method to analyze skin micro-relief using the images taken by smartphone's camera, which

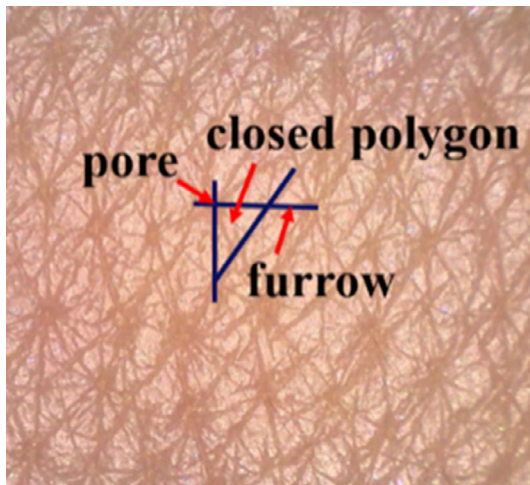


FIGURE 1 Skin micro-relief illustration

has the weakness of low resolution and unstable environment influence. These methods are either messy or need high resolution and expensive equipment. On the other hand, image processing algorithm development depends on the image type and resolution.

Skin micro-relief belongs to one series of texture. For the purpose of texture feature extraction from two-dimensional static images, analysis methods are categorized into seven classes: statistical way, structural way, transform-based way, model-based way, graph-based way, learning-based way, and entropy-based way.<sup>7</sup> Commonly used image analysis methods in skin micro-relief include grey level co-occurrence matrix (GLCM),<sup>8-10</sup> local binary pattern and variants(LBP)<sup>11</sup> which all belong to statistical way, and transform-based way comprising filter banks, Fourier transform, Gabor transform and so on. However, there's a common drawback among these methods, which has a shortage of relationship between proceeding results and visual results. Therefore, in this study, Tamura features algorithm is

used as the skin surface analysis method, which is first proposed by Tamura et al,<sup>12</sup> in 1978 and corresponded to visual perception. Howarth et al,<sup>13</sup> compared the evaluation using GLCM, the Tamura features and Gabor filters, and it turned out Tamura features had a better visually meaningful result.

This study aims to evaluate skin condition using skin micro-relief images quantitatively and comprehensively. We establish an image analysis method to extract the skin micro-relief related parameters, assess the most essential parameter among them and calculate the relationship. Also, we apply the method in researching age-related change.

## 2 | METHODS

### 2.1 | Image capture device

The skin micro-relief image is captured at the cheek by the microscope called SmartSkinCare<sup>®</sup> (IT Access Co., Ltd, Yokohama, Japan), with a camera, white LED lamps and UV-LED lamps (Figure 2). The operation consists of four steps. First of all, the microscope should connect the application to the smartphone or tablet and connect the Wi-Fi to use the cloud service. Secondly, make sure the light source and capture mode are appropriate since it has four modes to measure skin conditions, including skin micro-relief, color, porphyrins and sebum. After all the preparation been checked, the microscope should contact the skin vertically and softly so that the micro-relief image could be taken successfully. At last, the captured image could be displayed and exported. The area evaluated is 12 mm × 9 mm and the resolution of the image taken is 1280 × 960 pixels, with 23.7× magnification.

### 2.2 | Skin micro-relief image analysis methods

#### 2.2.1 | Pre-processing

Before image analysis, it is essential to pre-process the image avoiding the influence of noise and light, since two-dimensional skin micro-relief images are taken by the microscope, which is easily affected by the surrounding environment.

In the pre-processing step, the region of interest (ROI) is chosen as the center part of the original image, whose size is 800 × 800 pixels. Then B component image from RGB matrix is extracted as the basic image due to its sharpness. Light uniform algorithm was applied according to the method proposed by Zhang Q. et al,<sup>14</sup> which has four steps, (a) calculate the global average luminance ( $Lum_g$ ) of the grayscale image; (b) separate the grayscale image into sub-blocks and calculate their average luminance ( $Lum_l$ ) and gain the luminance difference matrix D, which is calculated by the formula:

$$\Delta_{lum} = Lum_l - Lum_g \quad (1)$$

(c) Interpolation algorithm for matrix D until element numbers equal to 800 × 800; (d) Merge matrix D and grayscale image into a

new image, whose size is 800 × 800 pixels. Finally, the uniformed grayscale ROI is gotten (Figure 3).

the child group, informed consent was obtained from their parents. Images were captured on the cheek of volunteers without any makeup.

### 2.2.2 | Skin parameters extraction and calculation

As shown in Figure 4 4 aspects and 11 skin parameters are separated from the original image with different image processing algorithms according to the properties of skin micro-relief, which are skin surface (coarseness, contrast and directionality), skin pores (number, area and average area), skin furrows (length and width) and the skin closed polygons (number, area and average area). The details of processing algorithms are shown in the results part.

### 2.3 | Study population and design

In this study, a total of 163 healthy Japanese female volunteers between 0 and 70 years old were enrolled. These females were divided into six groups: (a) 0-10 years old, (b) 20-30 years old, (c) 30-40 years old, (d) 40-50 years old, (e) 50-60 years old, and (f) 60-70 years old. The subjects number and mean age of each group are shown in Table 1. The study was conducted according to the principles of the declaration of Helsinki. Informed consent was obtained from all the subjects after the subjects were providing a complete explanation of the protocol. In the case of

### 2.4 | Statistical analysis

SPSS 21.0 (SPSS Science, Chicago, IL) software was used for all statistical analyses. All data were expressed as the mean SD (standard deviation). Pearson correlation coefficients were assessed between the age and all parameters. The linear fitting model was applied to analyze the trends of parameters with age. The correlation among all parameters was calculated by Pearson correlation coefficients, which lower than 0.3 representing weak correlation, 0.4-0.6 representing mediate correlation and higher than 0.6 representing high correlation. The statistical tests were two-tailed with the following significance levels:  $P < .05$  and  $P < .01$ .

## 3 | RESULTS

### 3.1 | Skin micro-relief features extraction

Two-dimensional skin micro-relief image was preprocessed first in order to analyze skin surface features and extract pores, furrows and closed polygons of the skin surface.

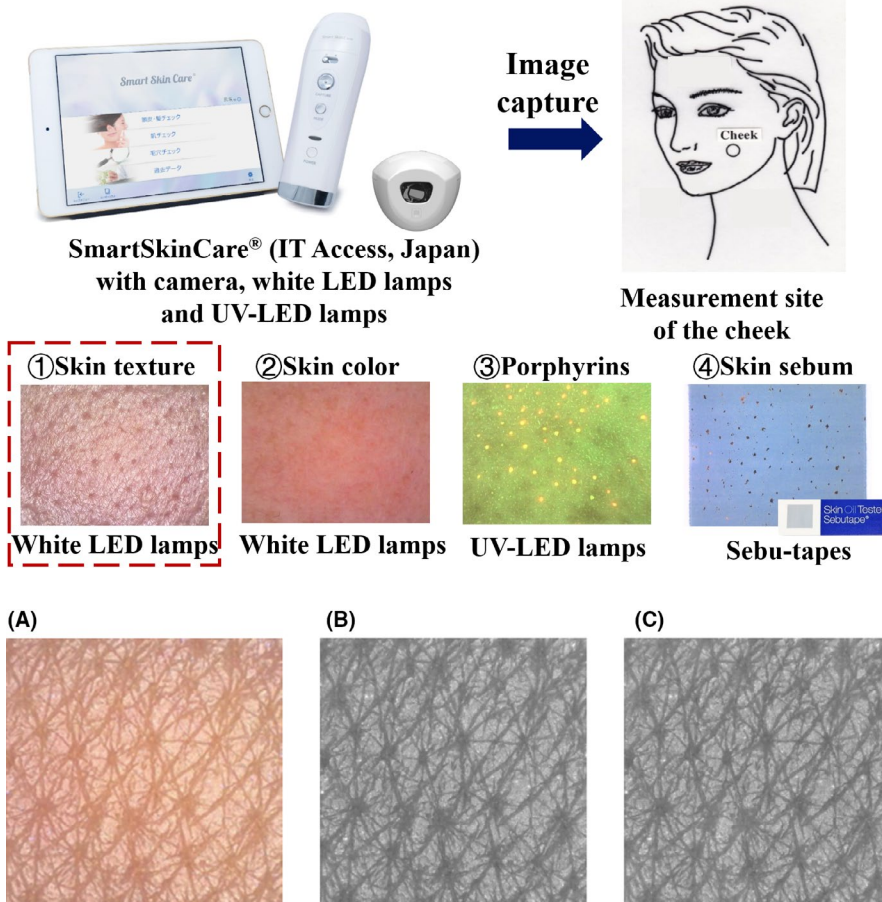
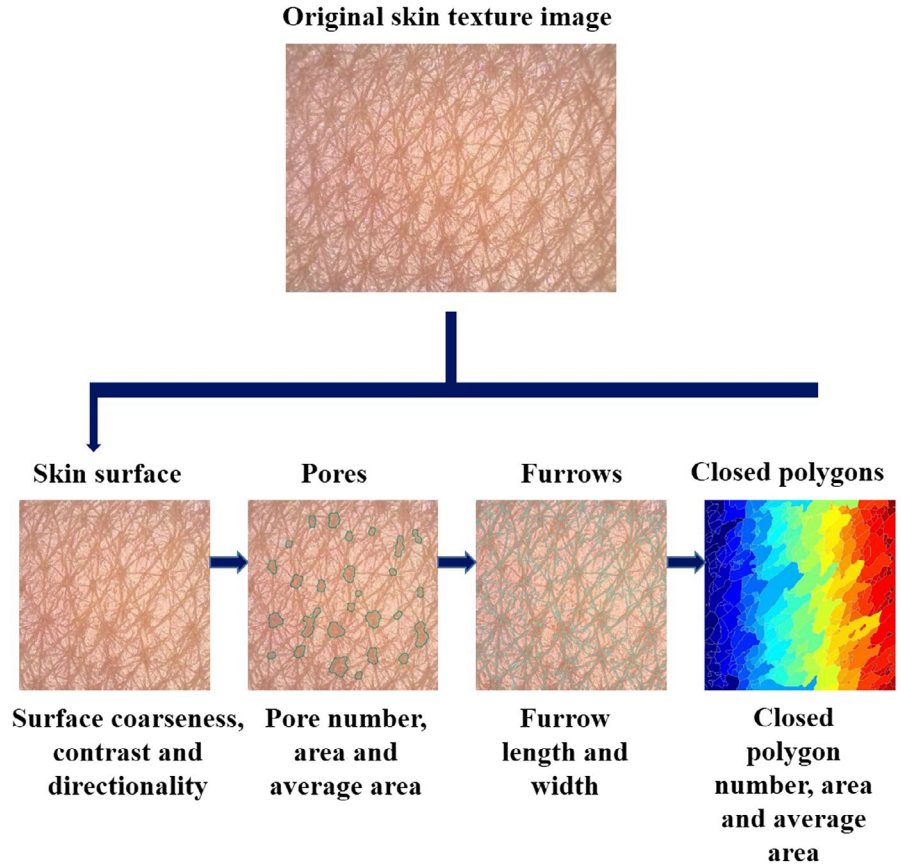


FIGURE 2 Skin image capture operation

FIGURE 3 Pre-processing illustration (A) original image, (B) B image, (C) light uniformed image

**FIGURE 4** FIGURE Skin micro-relief evaluation flowchart



**TABLE 1** Subject information

Age group	0s	20s	30s	40s	50s	60s	Sum
Number	21	31	29	29	32	21	163
Mean age	5.10 ± 0.62	24.90 ± 1.19	34.86 ± 0.58	44.86 ± 0.74	53.69 ± 1.75	64.86 ± 1.15	

### 3.1.1 | Skin surface

The flowchart of skin surface extraction is shown in Figure 5. It's worth noting that for the purpose of evaluating the skin surface, Tamura features algorithm was applied to extract skin surface features, including coarseness, contrast and directionality, which are the most commonly used features calculated by Tamura features algorithm. Tamura features algorithm is proposed by Tamura et al,<sup>12</sup> to correspond to visual perception. For an image  $f$  with size  $m \times n$ , and the pixel at location  $x$  and  $y$  as  $f(x,y)$ .

(a) Coarseness: The bigger its element size and/or the less its elements are repeated, the coarser it is felt.

STEP 1. take averages of every point over neighborhoods, the size is  $2^k$ .

$$A_k(x, y) = \sum_{i=x-2^{k-1}}^{x+2^{k-1}-1} \sum_{j=y-2^{k-1}}^{y+2^{k-1}-1} f(i, j) / 2^{2k} \quad (2)$$

STEP 2. take differences of horizontal and vertical sides for each point.

$$E_{k,h}(x, y) = \left| A_k(x + 2^{k-1}, y) - A_k(x - 2^{k-1}, y) \right| \quad (3)$$

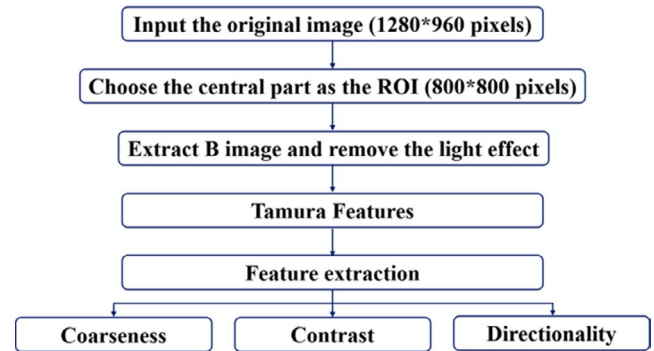


**FIGURE 5** Flowchart of skin surface extraction

$$E_{k,v}(x, y) = \left| A_k(x, y + 2^{k-1}) - A_k(x, y - 2^{k-1}) \right| \quad (4)$$

STEP 3. At each point, pick the best size which gives the highest output value.

$$S_{\text{best}}(x, y) = 2^k; E_k = E_{\text{max}} = \max(E_1, E_2, \dots, E_n) \quad (5)$$

STEP 4. take the average of  $S_{best}$  over the image.

$$F_{crs} = \frac{1}{m \times n} \sum_i^m \sum_j^n S_{best}(i, j) \quad (6)$$

(b) Contrast: The larger the range of gray-scale values, the higher the contrast is. Gray-scale "histogram flattening" transformation is said to be used for the purpose of removing the effects of unequal overall brightness and contrast in the original images.

$$F_{con} = \frac{\sigma}{\alpha^{1/4}}; \alpha_4 = \frac{\mu_4}{\sigma^4} \quad (7)$$

$\sigma^2$ : standard variance of gray-levels;  $\mu_4$ : the fourth moment about the mean;  $\alpha_4$ : the kurtosis as the index of polarization.

(c) Directionality: Directionality in an original picture usually can be preserved in its Fourier power spectrum, but it is time-consuming. This method utilizes the fact that gradient is a vector, so it has both magnitude  $\Delta G$  and local edge direction  $\theta$ .

$$|\Delta G| = \frac{|\Delta_H| + |\Delta_V|}{2}; \theta = \tan^{-1} \left( \frac{\Delta_V}{\Delta_H} \right) + \frac{\pi}{2} \quad (8)$$

$\Delta_H$ : horizontal differences measured by  $3 \times 3$  operator 1.

$\Delta_V$ : vertical differences measured by  $3 \times 3$  operator 2.

$$H_D(k) = \frac{N_\theta(k)}{\sum_{i=0}^{n-1} N_\theta(i)}, k = 0, 1, \dots, n-1 \quad (9)$$

operator 1:

-1	0	1
-1	0	1
-1	0	1

operator 2:

1	1	1
0	0	0
-1	-1	-1

$H_D$ : the desired histogram obtained by quantizing  $\theta$  and counting the points with  $\Delta G$ .

$$F_{dir} = \sum_p^{n_p} \sum_{\phi \in wp} (\phi - \phi)^2 H_D(\phi) \quad (10)$$

$n_p$ : the number of peaks;  $\phi_p$ :  $p^{\text{th}}$  peak position of  $H_D$ ;  $w_p$ : the range of  $p^{\text{th}}$  peak between valleys.

### 3.1.2 | Skin pores

In an attempt to calculate skin pore number and area, Otsu's method was applied primarily to choose a threshold from the

grayscale image and convert it to a binary image. Then close and open morphology transforms were combined to identify skin pore candidates using a disk-shaped structuring element, whose radius is 12. From the inverse image of the skin pore candidates, areas smaller than 500 pixels and bigger than 8000 pixels were eliminated and those connected to the image border were also removed. Finally, real pores were identified and features of pores were calculated, which are pore number, area, and average area (Figure 6).

### 3.1.3 | Skin furrow

The flowchart of skin furrow segmentation is shown in Figure 7. Watershed transform was used as the main algorithm to extract skin

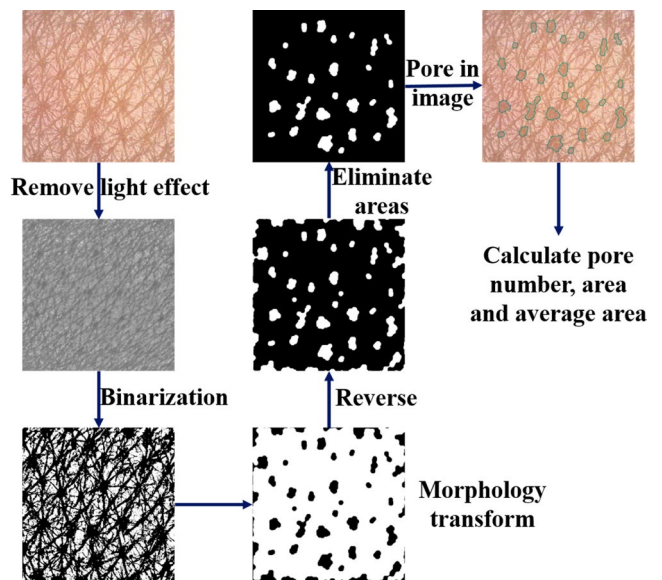


FIGURE 6 Flowchart of skin pore classification

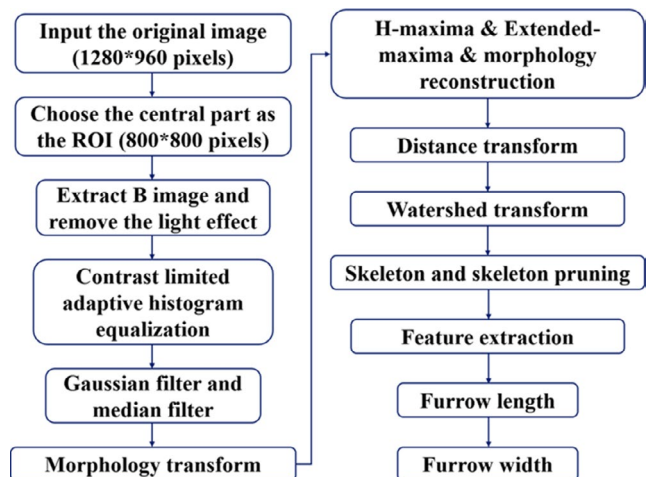
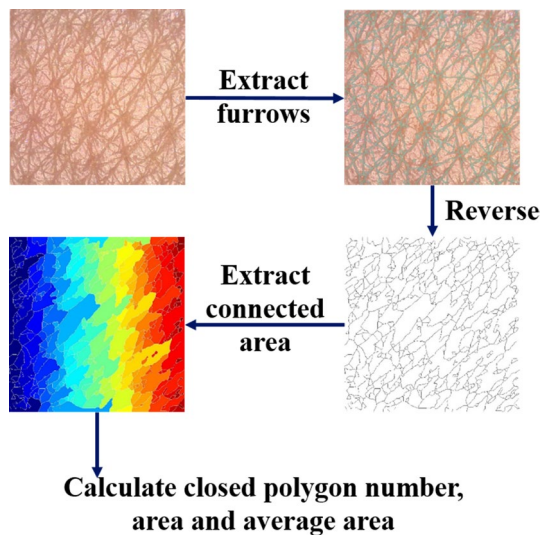


FIGURE 7 Flowchart of skin furrow extraction

furrow. Due to the properties of the Watershed transform, some pre-processing steps are necessary in case of over-segmentation. Contrast limited adaptive histogram equalization (CLAHE) was used to enhance the details of the image, which caused some noise also remarkable. Therefore, Gaussian filter as the linear smoothing filter and median filter as the non-linear smoothing filter were applied to remove the noise. For the purpose of obtaining the huge contrast image between furrows and closed polygons, the top-hat and bottom-hat transforms were operated orderly and the top-hat image was added into the median filtered image and the bottom-hat image was subtracted from it. H-maxima transforms, extended maxima transform and morphology reconstruction were applied to acquire the binary image. Distance transform and watershed transform were used to get the furrow candidates. Identified pores were eliminated and skeleton pruning was used to suppress the extra lines other than furrows. Skeleton operation in morphological transform was used



**FIGURE 8** Skin furrow extraction illustration, (A) watershed transform result; (B) skin furrow extraction; (C) skin furrow area extraction without pores

five times to get a suitable furrow area. In the end, furrow length was calculated and furrow width was got by furrow area dividing by furrow length (Figure 8).

### 3.1.4 | Skin closed polygon

Since skin furrow has been extracted, skin closed polygons were extracted by reversing furrow image with labeling (Figure 9), closed polygon number, area, and average area were calculated.

## 3.2 | Age-dependent changes with skin micro-relief

Age-dependent changes in the skin surface, pore, furrow, and closed polygon were examined and results are shown in Figure 10. In the skin surface, all parameters increased with age, especially coarseness and contrast with significant differences. Skin pore number, area, and average area increased with age with significant differences, which indicates that skin pores become larger and more obvious with age went on. Skin furrow length decreased with age, while width increased with age. Skin closed polygon number decreases with age, however, their area and average area increase with age. According to the coefficient of correlation between age and all parameters, the relevance rank is contrast > closed polygon area > furrow length > coarseness > pore average area > furrow width > pore area > closed polygon number > closed polygon average area > pore number > directionality.

### 3.3 | Correlation among skin micro-relief related parameters

The correlation among all parameters is shown in Figure 11, in which surface directionality didn't have any correlation with other parameters. In contrast, pore average area and furrow

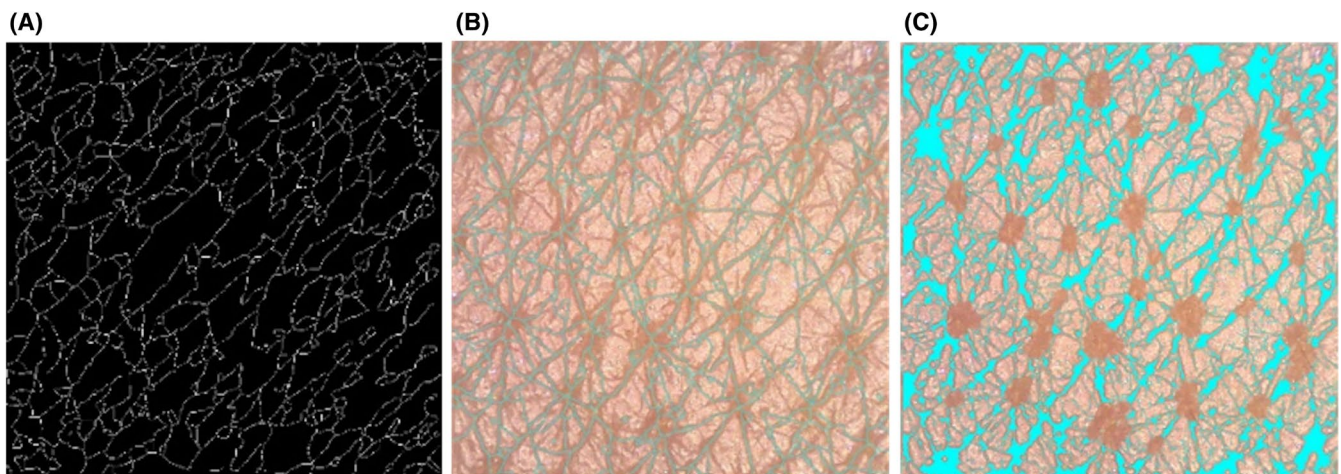


**FIGURE 9** Flowchart of skin closed polygon extraction

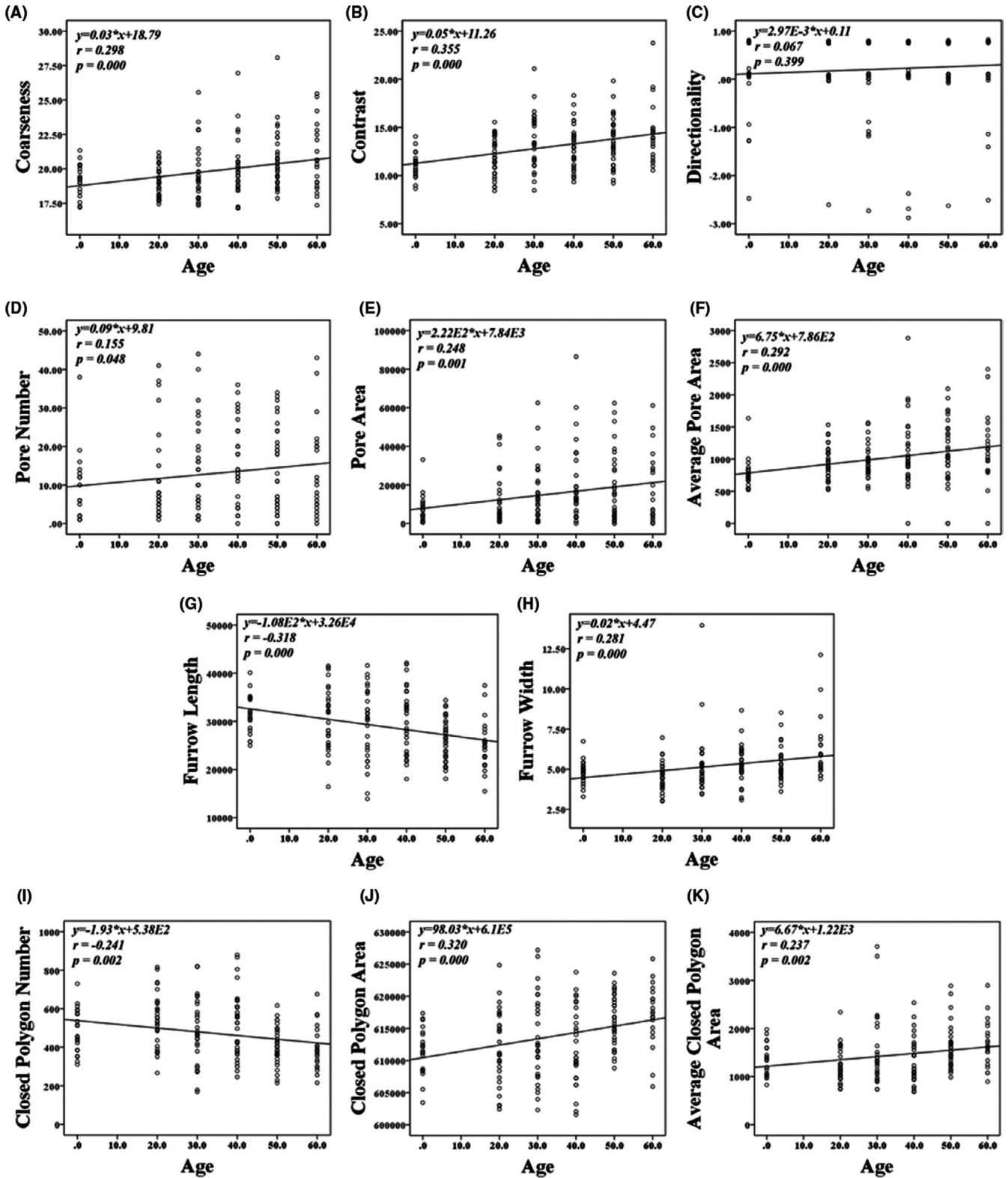
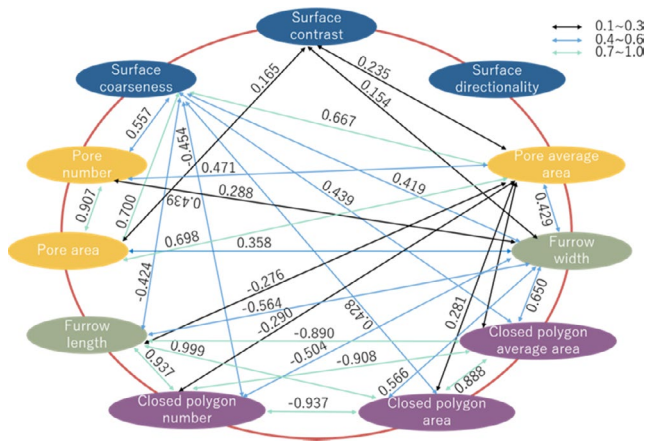


FIGURE 10 FIGURE Skin micro-relief parameters changes with age, (A) skin surface coarseness; (B) skin surface contrast; (C) skin surface directionality; (D) skin pore number; (E) skin pore area; (F) skin pore average area; (G) skin furrow length; (H) skin furrow width; (I) skin closed polygon number; (J) skin closed polygon area; (K) skin closed polygon average area

width have the most correlation with others, which indicated that these two parameters should be improved first if people want to refine their skin micro-relief conditions. In addition, the pore

area and pore average area have a strong correlation with skin coarseness, which implies larger the pore area is, the worse skin coarseness is.



**FIGURE 11** Relationships among parameters with significant differences: black lines represent the weak correlation; blue lines represent the mediate correlation; green lines represent the high correlation

## 4 | DISCUSSION

In this study, we proposed a skin micro-relief condition evaluation method by extracting skin pores, furrows, and closed polygons and analyzing the features of the two-dimensional image taken from the cheek position by the microscope. What's more, we employed this method to evaluate age-related changes and explored the relationships among parameters. All-sided indexes of skin micro-relief, including skin surface, pores, furrows, and closed polygons, been extracted and analyzed into 11 precise quantitative parameters from one image is a key point of skin micro-relief assessment.

As mentioned in the literature review, there are many algorithms and parameters could be used to evaluate skin micro-relief condition. Uchida et al,<sup>15</sup> used a short line matching method to extract skin furrows and assessed the changes as piloerection becoming weak in order to estimate emotion. C. I. Moon et al,<sup>6</sup> and Zou et al,<sup>4</sup> also used the watershed transform to extract skin closed polygons, but they didn't extract skin pores, which could also affect skin micro-relief condition evaluation.

PM Arabi et al,<sup>10</sup> compared GLCM and pixel intensity methods for skin texture analysis, and they believed pixel intensity is more useful and accurate. While in this research, considering the image type and resolution, and for the purpose of fitting human visual perception, Tamura features algorithm was applied in the study.

As we have known, the older human is, the rougher skin is. However, the concrete mechanism is still under exploration. In the study, we found out that as pores getting more obvious, furrow length decreasing, furrow width becoming larger, and small closed polygons merging into large ones, the skin is seen rougher than before. Jung HJ et al,<sup>16</sup> also performed that pore counts increased with age and the increment was huge between 30s and 40s years, while there is no significant difference by gender. Lee SJ et al,<sup>17</sup> reviewed the major causes of pores enlargement, which includes high sebum excretion, decreased elasticity around pores and increased

hair follicle volume. With age increasing, skin elasticity decreases significantly, which results in pore number and area increasing found in this study.

Skin furrow includes primary furrows (20-200  $\mu\text{m}$ ) and finer secondary furrows (30-70  $\mu\text{m}$ ), these furrows construct the triangle-shaped closed polygons originally. With age went on, especially the position exposed by sun, such as cheek, photo-aging also causes severe changes in the skin, like the lower expression of collagen production.<sup>18</sup> Kim et al,<sup>19</sup> also found out that skin furrow width of forearm and hand increased with age with dermoscopy and SEM. It can be understood that primary furrows become deeper and this phenomenon reduces the number of skin closed polygons and enlarges the area of skin closed polygons.

For the correlation among skin micro-relief related parameters, the correlation is strong between skin coarseness and skin pore area. Therefore, it is considered that all parameters deteriorating caused skin roughness, however, the major factor could be attributed to pores enlargement, which provides further support for the skin condition comparison according to age, gender or anatomic sites.

Compared to conventional methods, it has more potential to establish evaluation standards of skin surface micro-relief using the proposed method in the study. Using the same device makes sure all images have the same magnification of skin and resolution. In addition, the proposed algorithm divides skin surface micro-relief into four sections quantitatively, especially the objective and quantitative surface evaluation which was usually decided by human vision, such as roughness.

## 5 | CONCLUSION

This project was undertaken to design an objective and quantitative method from two-dimensional skin images using image analysis technology to evaluate skin micro-relief conditions comprehensively. The study confirmed skin micro-relief conditions get worse with age increases. For skin coarseness, skin pores enlargement is the most important factor. It has been proved the method proposed is an effective tool to evaluate skin aging. It is possible to assist dermatologist to diagnose and assess the therapeutic progress using the proposed method, such as eczema, which usually occurs adjoint sandpaper-like texture. In other words, this evaluation method of skin micro-relief from 2D images can be a powerful tool for cosmetic developers assessing skincare products, especially for skin anti-aging products. And it could also be used for customers to trace their skin changes.

In the future, the results of this method should be compared with visual perceptions. More skin parameters should be involved to evaluate skin conditions comprehensively.

## ORCID

Yue Wu  <https://orcid.org/0000-0001-8805-5388>



## REFERENCES

1. Akimoto M, Ikeda N, Maeda S, Watanabe M, Tokyo KM. Evaluation method of skin surface condition using image analysis. *Xxx*. 2016;16:3-5. (Japanese). [https://www.jstage.jst.go.jp/article/jacc/59/0/59\\_708/\\_pdf](https://www.jstage.jst.go.jp/article/jacc/59/0/59_708/_pdf)
2. Masuda Y, Oguri M, Morinaga T, Hirao T. Three-dimensional morphological characterization of the skin surface micro-topography using a skin replica and changes with age. *Ski Res Technol*. 2014;20(3):299-306. <https://doi.org/10.1111/srt.12119>
3. Maia Campos PMBG, Melo MO, Mercurio DG. Use of advanced imaging techniques for the characterization of oily skin. *Front Physiol*. 2019;10:1-9. <https://doi.org/10.3389/fphys.2019.00254>
4. Zou Y, Song E, Jin R. Age-dependent changes in skin surface assessed by a novel two-dimensional image analysis. *Ski Res Technol*. 2009;15(4):399-406. <https://doi.org/10.1111/j.1600-0846.2009.00377.x>
5. Bontozoglou C, Zhang X, Xiao P. Micro-relief analysis with skin capacitive imaging. *Ski Res Technol*. 2019;25(2):165-170. <https://doi.org/10.1111/srt.12628>
6. Moon CI, Lee O. Age-dependent skin texture analysis and evaluation using mobile camera image. *Ski Res Technol*. 2018;24(3):490-498. <https://doi.org/10.1111/srt.12459>
7. Humeau-Heurtier A. Texture feature extraction methods: a survey. *IEEE Access*. 2019;7:8975-9000. <https://doi.org/10.1109/ACCESS.2018.2890743>
8. Pang H, Chen T, Wang X, Chang Z, Shao S, Zhao J. Quantitative evaluation methods of skin condition based on texture feature parameters. *Saudi J Biol Sci*. 2017;24(3):514-518. <https://doi.org/10.1016/j.sjbs.2017.01.021>
9. Damanpreet Kaur PS. Human skin texture analysis using image processing techniques. *Int J Sci Res*. 2013;2(5):17-20. <https://www.ijsr.net/archive/v2i5/IJSROFF2013212.pdf>
10. Arabi PM, Joshi G, Vamsha DN. Performance evaluation of GLCM and pixel intensity matrix for skin texture analysis. *Perspect Sci*. 2016;8:203-206. <https://doi.org/10.1016/j.pisc.2016.03.018>
11. Singh R, Shah P, Bagade J. Skin texture analysis using machine learning. *Conf Adv Signal Process*. 2016;2016:494-497. <https://doi.org/10.1109/CASP.2016.7746222>
12. Tamura H, Mori S, Yamawaki T. Textural features corresponding to visual perception. *IEEE Trans Syst Man Cybern*. 1978;8(6):460-473. <https://doi.org/10.1109/TSMC.1978.4309999>
13. Howarth P, R ger S. Evaluation of texture features for content-based image retrieval. *Lect Notes Comput Sci (including Subser Lect Notes Artif Intell Lect Notes Bioinformatics)*. 2004;3115:326-334. [https://doi.org/10.1007/978-3-540-27814-6\\_40](https://doi.org/10.1007/978-3-540-27814-6_40)
14. Zhang Q, Whangbo T. Skin pores detection for image-based skin analysis. 2008:233-240. [https://doi.org/10.1007/978-3-540-88906-9\\_30](https://doi.org/10.1007/978-3-540-88906-9_30)
15. Uchida M, Akaho R, Ogawa-Ochiai K, Tsumura N. Image-based measurement of changes to skin texture using piloerection for emotion estimation. *Artif Life Robot*. 2018;24(1):1-7. <https://doi.org/10.1007/s10015-018-0435-0>
16. Jung HJ, Ahn JY, Lee JI, et al. Analysis of the number of enlarged pores according to site, age, and sex. *Ski Res Technol*. 2018;24(3):367-370. <https://doi.org/10.1111/srt.12438>
17. Lee SJ, Seok J, Jeong SY, Park KY, Li K, Seo SJ. Facial pores: definition, causes, and treatment options. *Dermatologic Surg*. 2016;42(3):277-285. <https://doi.org/10.1097/DSS.0000000000000657>
18. Rabe JH, Mamelak AJ, McElgunn PJS, Morison WL, Sauder DN. Photoaging: mechanisms and repair. *J Am Acad Dermatol*. 2006;55(1):1-19. <https://doi.org/10.1016/j.jaad.2005.05.010>
19. Kim DH, Rhyu YS, Ahn HH, Hwang E, Uhm CS. Skin microrelief profiles as a cutaneous aging index. *Microscopy*. 2016;65(5):407-414. <https://doi.org/10.1093/jmicro/dfw019>

**How to cite this article:** Wu Y, Tanaka T. Objective and quantitative measurement of skin micro-relief by image analysis and application in age-dependent changes. *Skin Res Technol*. 2021;27:1072–1080. <https://doi.org/10.1111/srt.13060>